

Observation of the critical end point in the phase diagram for hot and dense nuclear matter

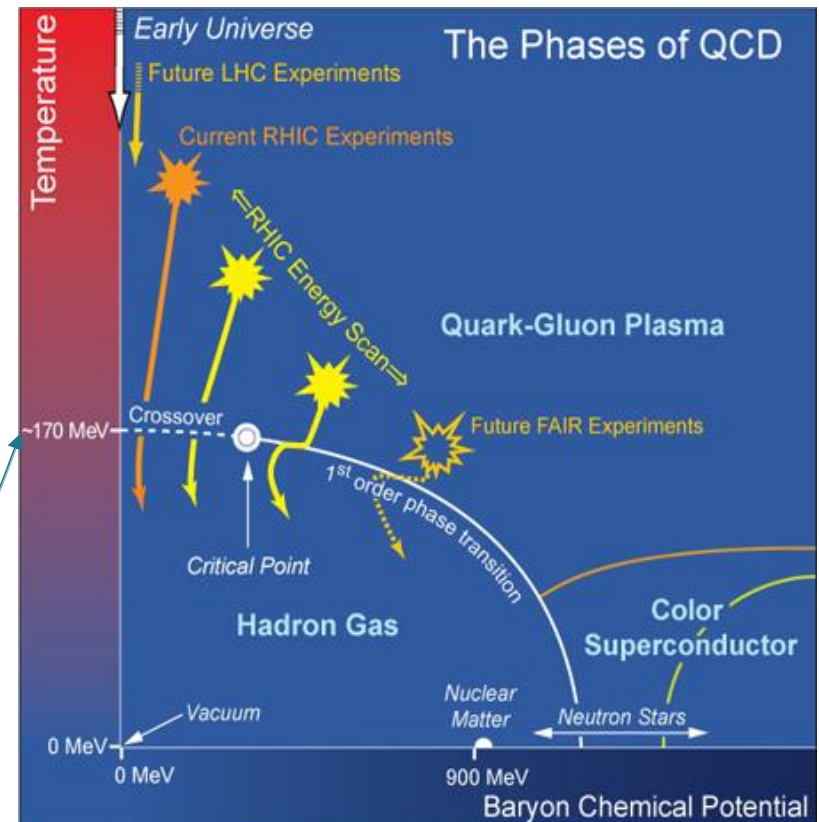
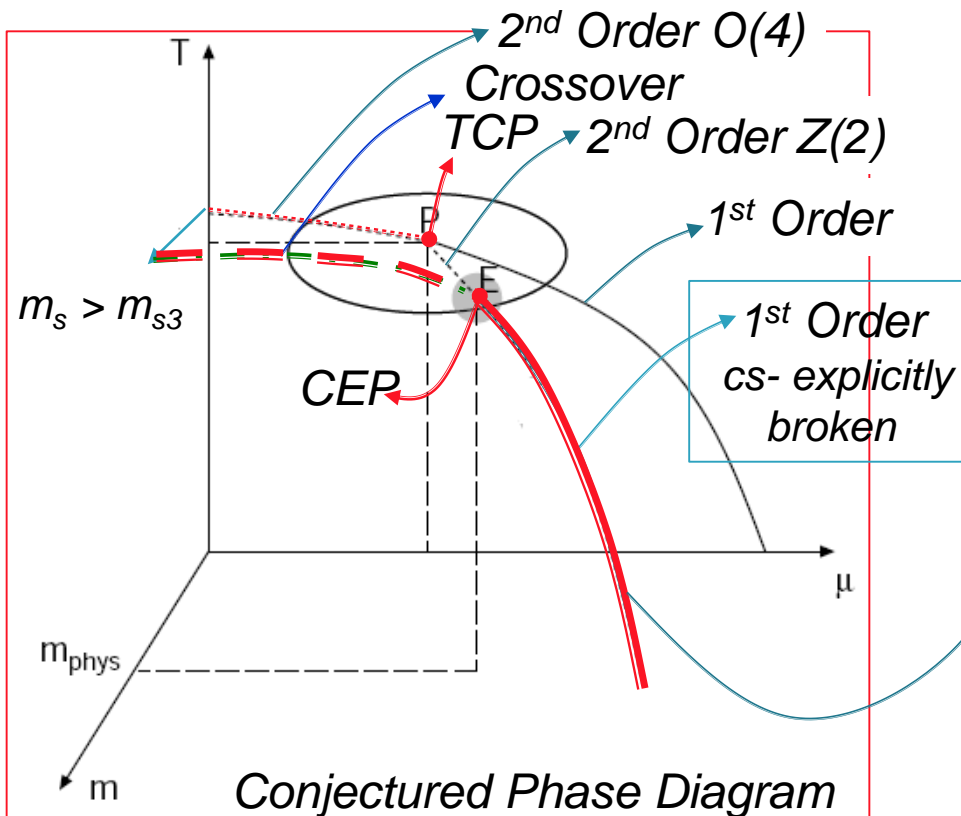
*Roy A. Lacey
Stony Brook University*

Outline

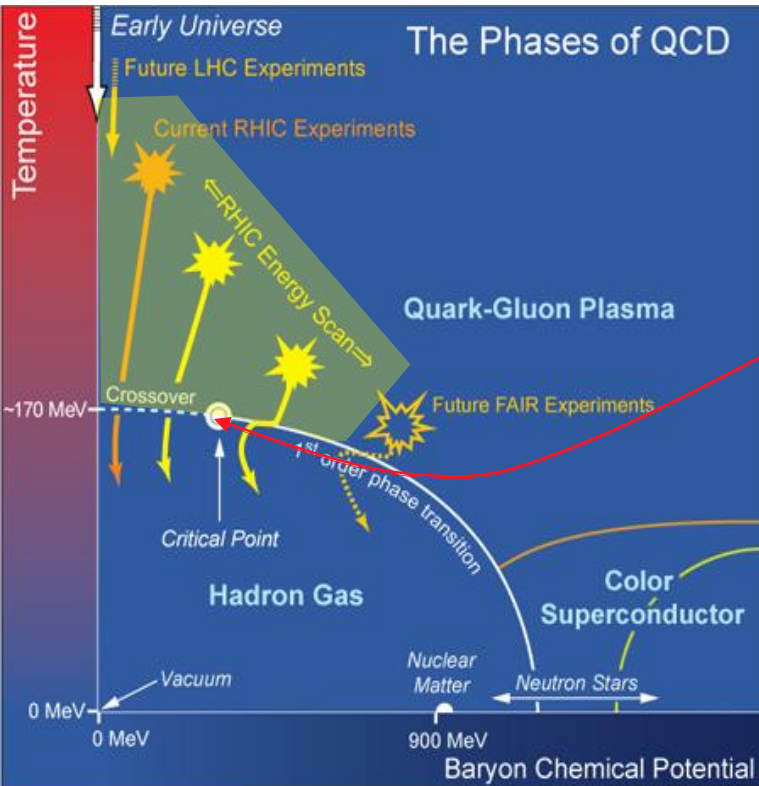
- **Introduction**
 - ✓ *Phase Diagrams & HIC*
- **Search strategy for the CEP**
 - ✓ *Theoretical guidance*
 - ✓ *Guiding principles for search*
- **The probe**
 - ✓ *Femtoscopic
“susceptibility”*
- **Analysis**
 - ✓ *Finite-Size-Scaling*
 - ✓ *Dynamic Finite-Size-Scaling*
- **Summary**
 - ✓ **Epilogue**

The QCD Phase Diagram

A central goal of the worldwide program in relativistic heavy ion collisions, is to chart the QCD phase diagram



The QCD Phase Diagram



Essential Question

What new insights do we have on:

The CEP “landmark”?

- ✓ Location (T^{cep}, μ_B^{cep}) values?
- ✓ Static critical exponents - ν, γ ?
 - Static universality class?
 - Order of the transition
- ✓ Dynamic critical exponent/s – z ?
 - Dynamic universality class?

All are required to fully characterize the CEP

Theoretical Guidance

Theory consensus on the static universality class for the CEP

3D-Ising Z(2)

✓ $\nu \sim 0.63$

✓ $\gamma \sim 1.2$

M. A. Stephanov

Int. J. Mod. Phys. A 20, 4387 (2005)

Dynamic Universality class for the CEP less clear

➤ One slow mode (L)

✓ $z \sim 3$ - Model H

Son & Stephanov

Phys.Rev. D70 (2004) 056001

Moore & Saremi,

JHEP 0809, 015 (2008)

➤ Three slow modes (NL)

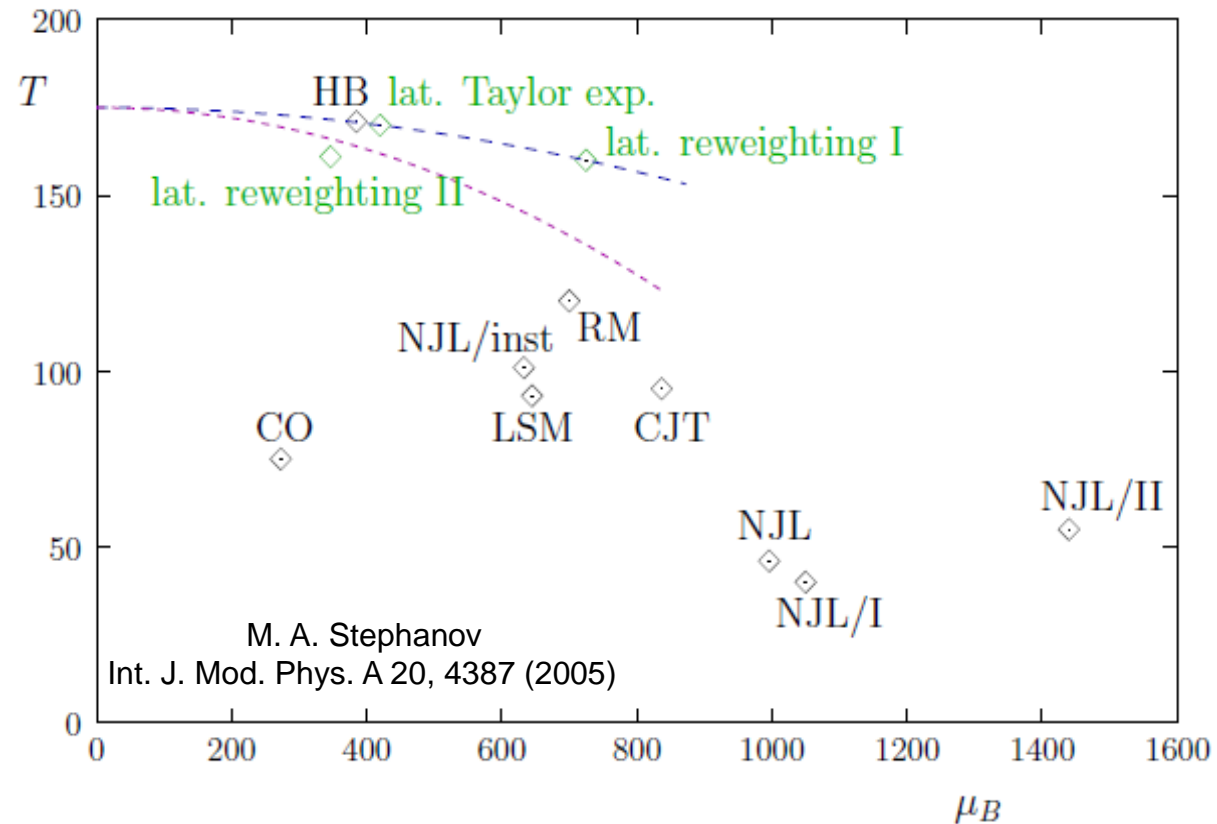
✓ $z_T \sim 3$

✓ $z_V \sim 2$

✓ $z_S \sim -0.8$

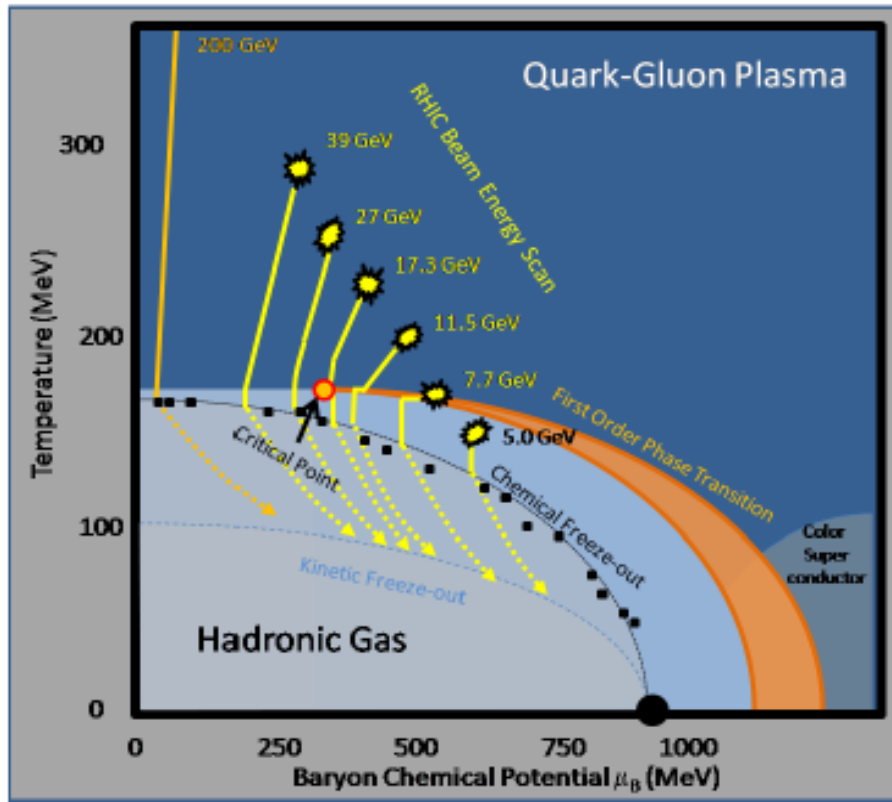
Y. Minami - Phys.Rev. D83
(2011) 094019

The predicted location ($T^{\text{cep}}, \mu_B^{\text{cep}}$) of the CEP is even less clear!



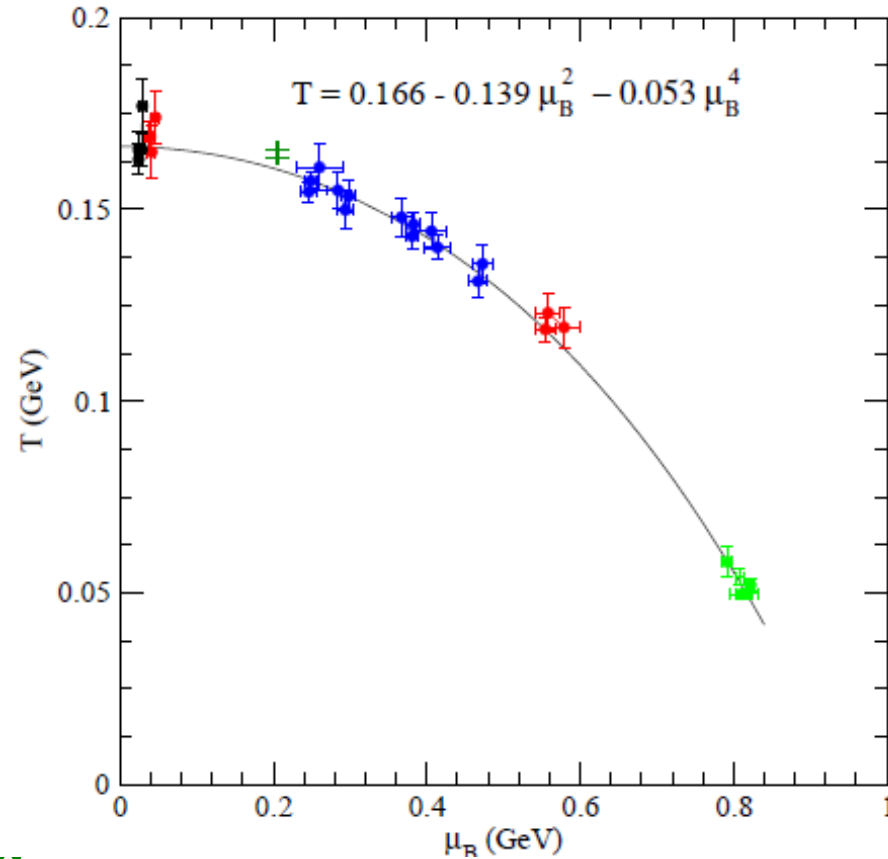
Experimental verification and characterization of the CEP is a crucial ingredient

RHIC-LHC (T, μ_B) Domain



- **LHC** → access to high T and small μ_B
- **RHIC** → access to different systems and a broad domain of the (μ_B, T) -plane

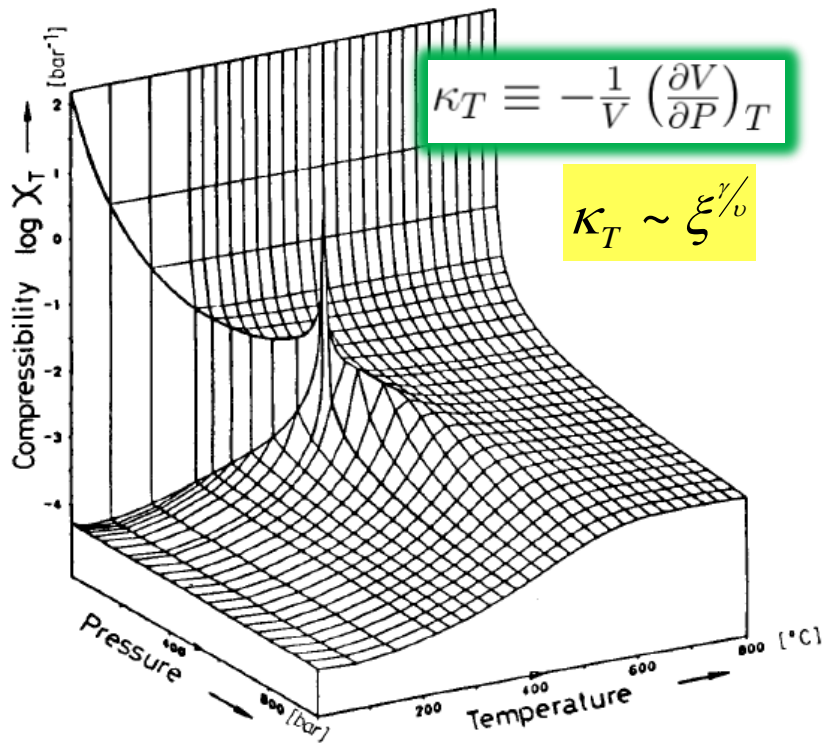
(μ_B, T) at chemical freeze-out



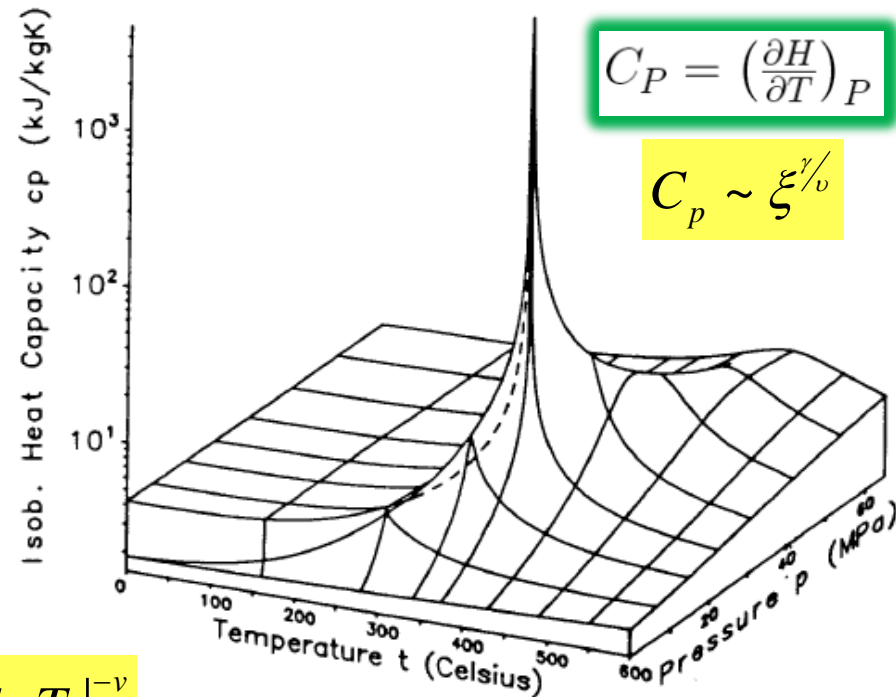
RHIC_{BES} to LHC → $\sim 360 \sqrt{s_{NN}}$ increase

$\sqrt{s_{NN}}$ is a good proxy for exploring the (T, μ_B) plane for Experimental signatures!

Anatomy of search strategy



H₂O



$\xi \sim |T - T_c|^{-\nu}$

➤ $\langle (\delta n) \rangle \sim \xi^2 \rightarrow$ search for “critical” fluctuations in HIC

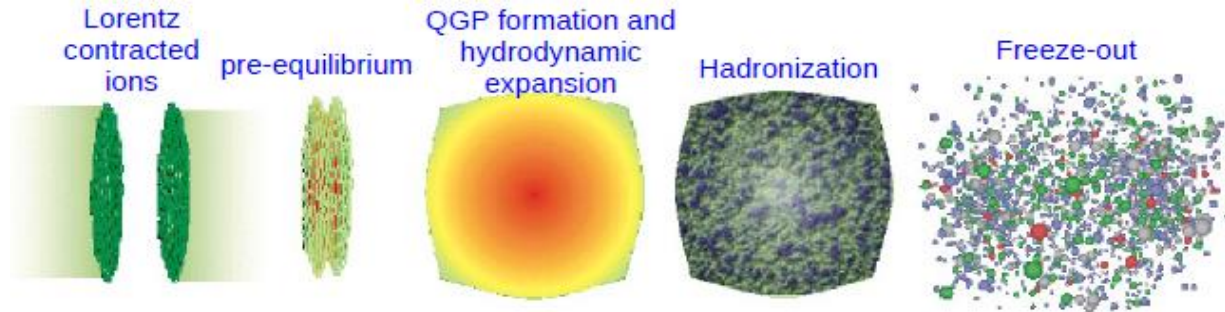
Stephanov, Rajagopal, Shuryak, PRL.81, 4816 (98)

The critical point is characterized by several (power law) divergences

Central idea → use beam energy scans to vary μ_B & T to search for the influence of such divergences!

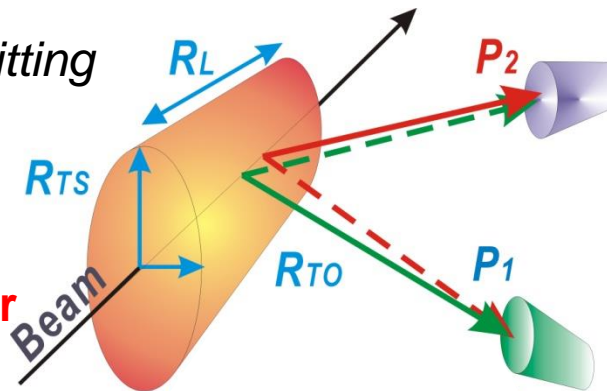
→ We use femtoscopic measurements to perform our search

Interferometry as a susceptibility probe



The expansion of the emitting source (R_L, R_{T0}, R_{TS}) produced in HI collisions is driven by c_s

χ of the order parameter diverges at the CEP



$$c_s^2 = \frac{1}{\rho\kappa}$$

← Susceptibility (χ)

In the vicinity of a phase transition or the CEP, the divergence of κ leads to anomalies in the expansion dynamics

Strategy

Search for non-monotonic patterns for HBT radii combinations that are sensitive to the divergence of κ

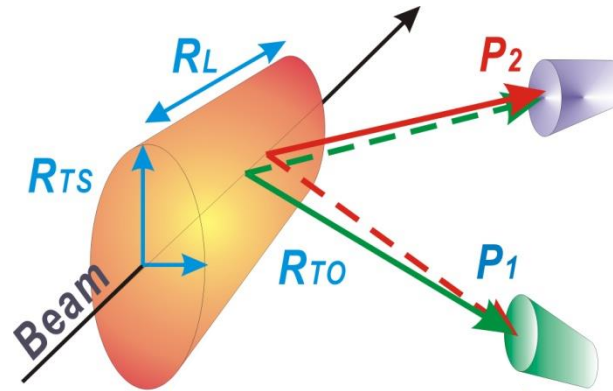
Measuring HBT Radii

Hanbury Brown & Twist (HBT) radii obtained from two-particle correlation functions

$$C(\mathbf{q}) = \frac{dN_2 / d\mathbf{p}_1 d\mathbf{p}_2}{(dN_1 / d\mathbf{p}_1)(dN_1 / d\mathbf{p}_2)}$$

$$\mathbf{q} = \mathbf{p}_2 - \mathbf{p}_1$$

S. Afanasiev et al.
PRL 100 (2008) 232301



3D Koonin Pratt Eqn.

$$R(\mathbf{q}) = C(\mathbf{q}) - 1 = 4\pi \int dr r^2 K_0(\mathbf{q}, r) S(r)$$

Correlation function

Encodes FSI

Source function
(Distribution of pair separations)

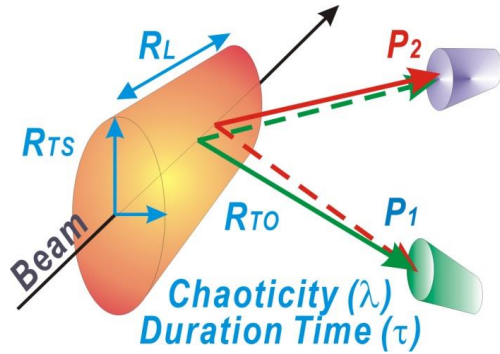
Inversion of this integral equation → **Source Function**
(R_L, R_{TO}, R_{TS})

$$c_s^2 = \frac{1}{\rho \kappa_s}$$

$$C_2(\mathbf{q}) = N[(\lambda(1 + G(\mathbf{q})))F_c + (1 - \lambda)],$$

$$G(\mathbf{q}) \cong \exp(-R_{\text{side}}^2 q_{\text{side}}^2 - R_{\text{out}}^2 q_{\text{out}}^2 - R_{\text{long}}^2 q_{\text{long}}^2).$$

Interferometry signal

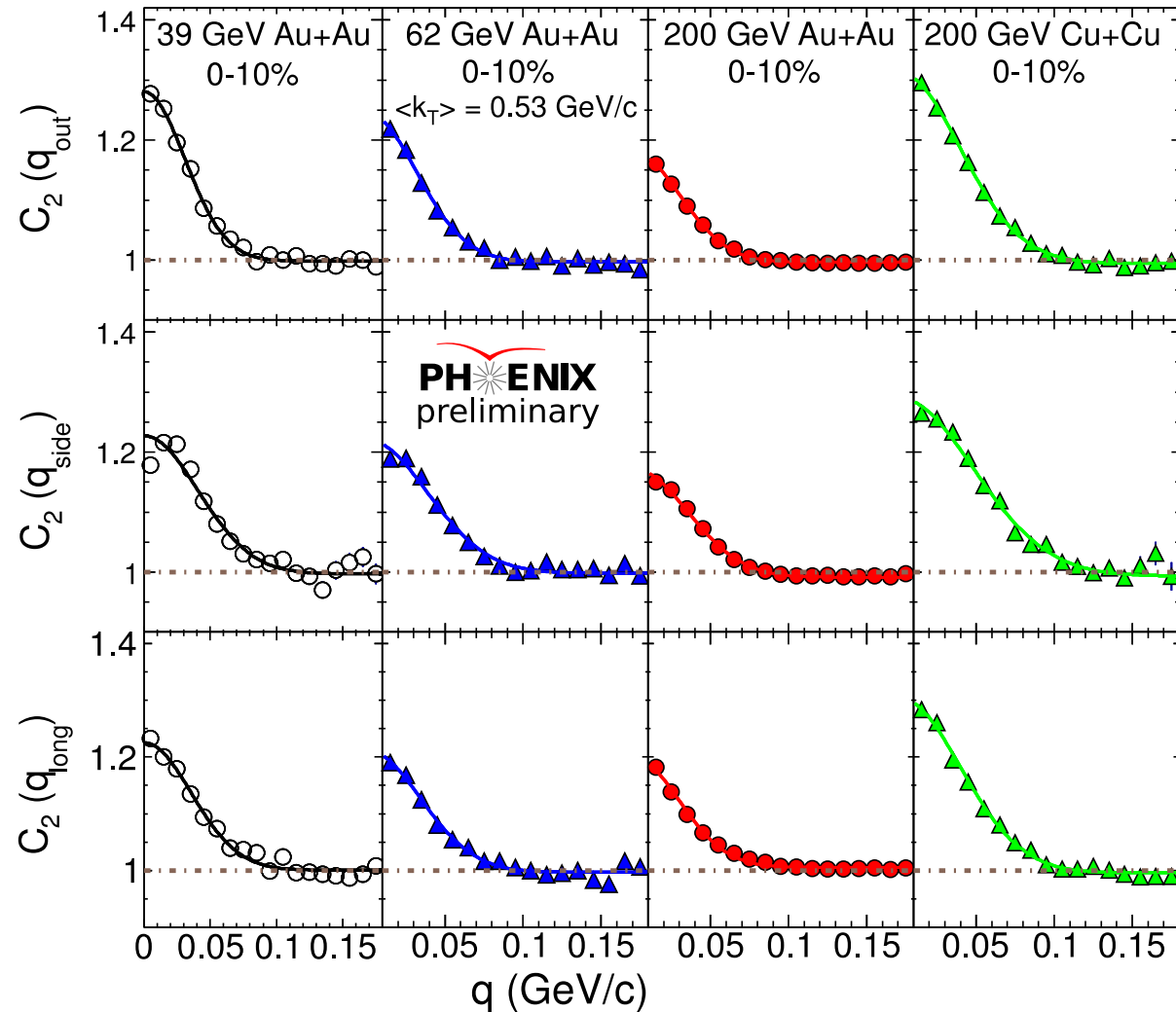


$$C(\mathbf{q}) = \frac{dN_2 / d\mathbf{p}_1 d\mathbf{p}_2}{(dN_1 / d\mathbf{p}_1)(dN_1 / d\mathbf{p}_2)}$$

Adare et. al. (PHENIX)

[arXiv:1410.2559](https://arxiv.org/abs/1410.2559)

Two pion correlation functions

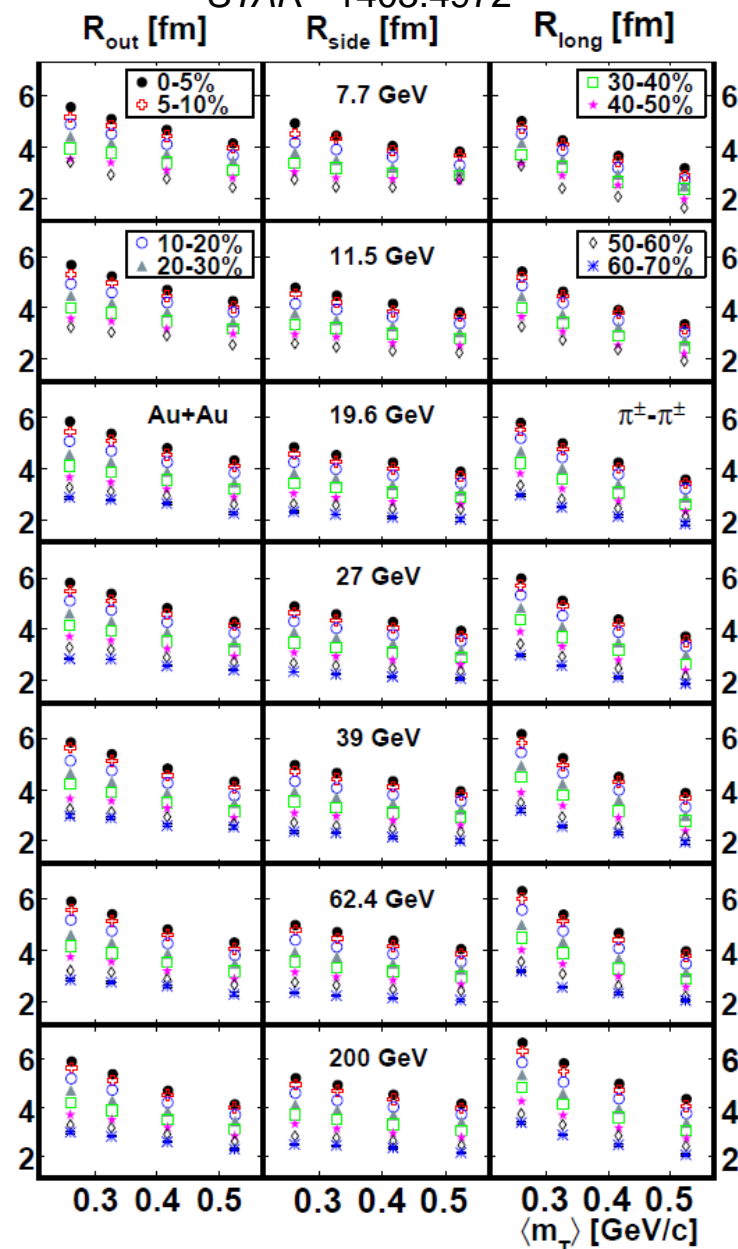
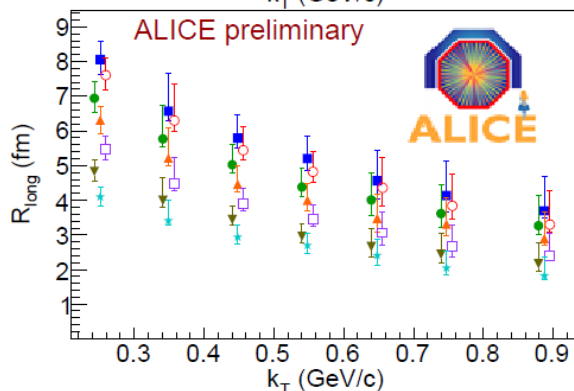
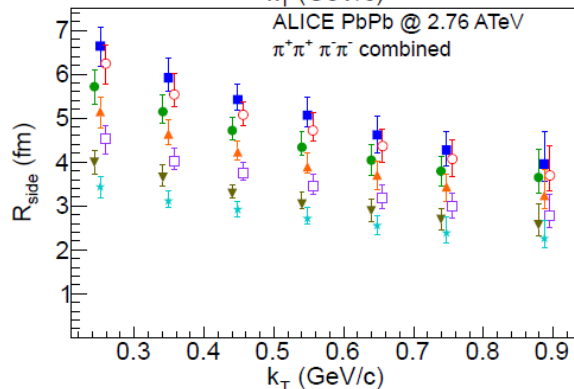
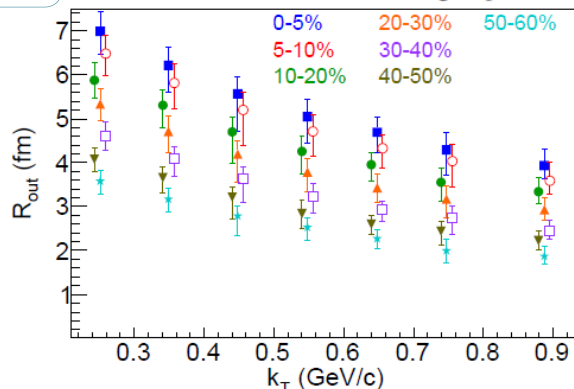


$$C_2(\mathbf{q}) = N[(\lambda(1 + G(\mathbf{q})))F_c + (1 - \lambda)],$$

$$G(\mathbf{q}) \cong \exp(-R_{\text{side}}^2 q_{\text{side}}^2 - R_{\text{out}}^2 q_{\text{out}}^2 - R_{\text{long}}^2 q_{\text{long}}^2).$$

HBT Measurements

ALICE -PoSWPCF2011



*This comprehensive
Set of two-pion
HBT measurements
is used for our search*

Strategy: Search for non-monotonic patterns for HBT radii combinations that are sensitive to the divergence of κ

Interferometry Probe

Hung, Shuryak, PRL. 75,4003 (95)

T. Csörgő. and B. Lörstad, PRC54 (1996) 1390-1403

Chapman, Scotto, Heinz, PRL.74.4400 (95)

Makhlin, Sinyukov, ZPC.39.69 (88)

$$R_{side}^2 = \frac{R_{geo}^2}{1 + \frac{m_T}{T} \beta_T^2}$$

$$R_{out}^2 = \frac{R_{geo}^2}{1 + \frac{m_T}{T} \beta_T^2} + \frac{\beta_T^2 (\Delta \tau)^2}{T}$$

$$R_{long}^2 \approx \frac{T}{m_T} \tau^2$$

emission duration

emission lifetime

$(R_{out}^2 - R_{side}^2)$ sensitive to the κ

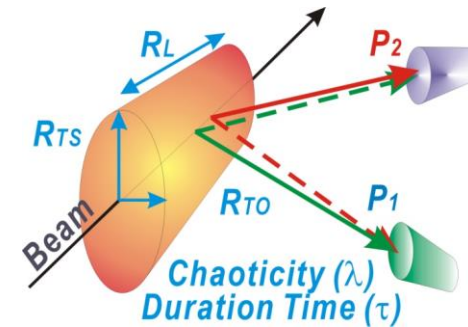
$(R_{side} - R_{init})/R_{long}$ sensitive to c_s

Specific non-monotonic patterns expected as a function of $\sqrt{s_{NN}}$

➤ A maximum for $(R_{out}^2 - R_{side}^2)$

➤ A minimum for $(R_{side} - R_{initial})/R_{long}$

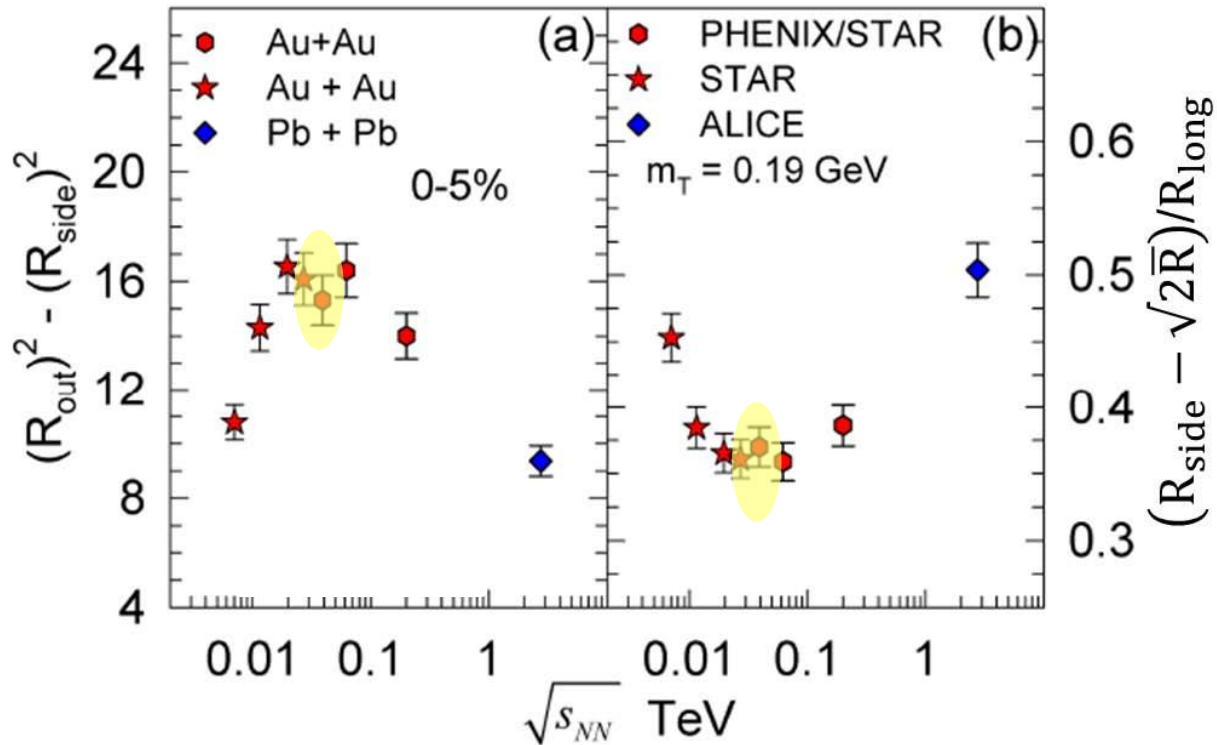
The measured HBT radii encode space-time information for the reaction dynamics



$$c_s^2 = \frac{1}{\rho \kappa}$$

The divergence of the susceptibility κ

- ✓ “softens” the sound speed c_s
- ✓ extends the emission duration



$$R_{long} \propto \tau$$

$$(R_{out}^2 - R_{side}^2) \propto \Delta \tau^2$$

$$(R_{side} - R_i) / R_{long} \propto u$$

$$R_{initial} = \sqrt{2\bar{R}}$$

The measurements validate the expected non-monotonic patterns!

→ Reaction trajectories spend a fair amount of time near a “soft point” in the EOS that coincides with the CEP!

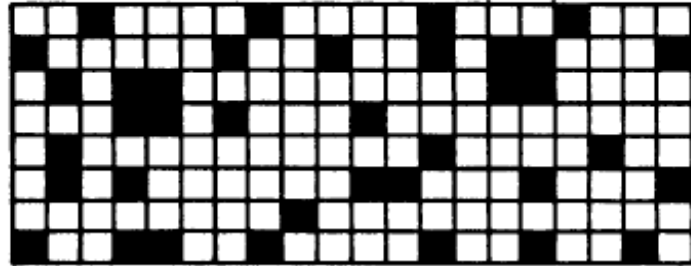
**** Note that R_{long} , R_{out} and R_{side} [all] increase with $\sqrt{s_{NN}}$ ****

Finite-Size Scaling (FSS) is used for further validation of the CEP, as well as to characterize its static and dynamic properties

Basis of Finite-Size Effects

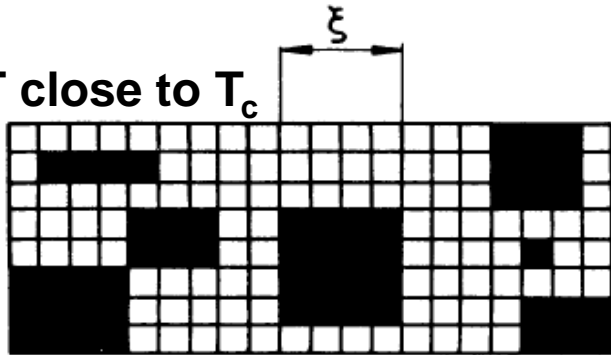
Illustration

$T > T_c$



L characterizes the system size

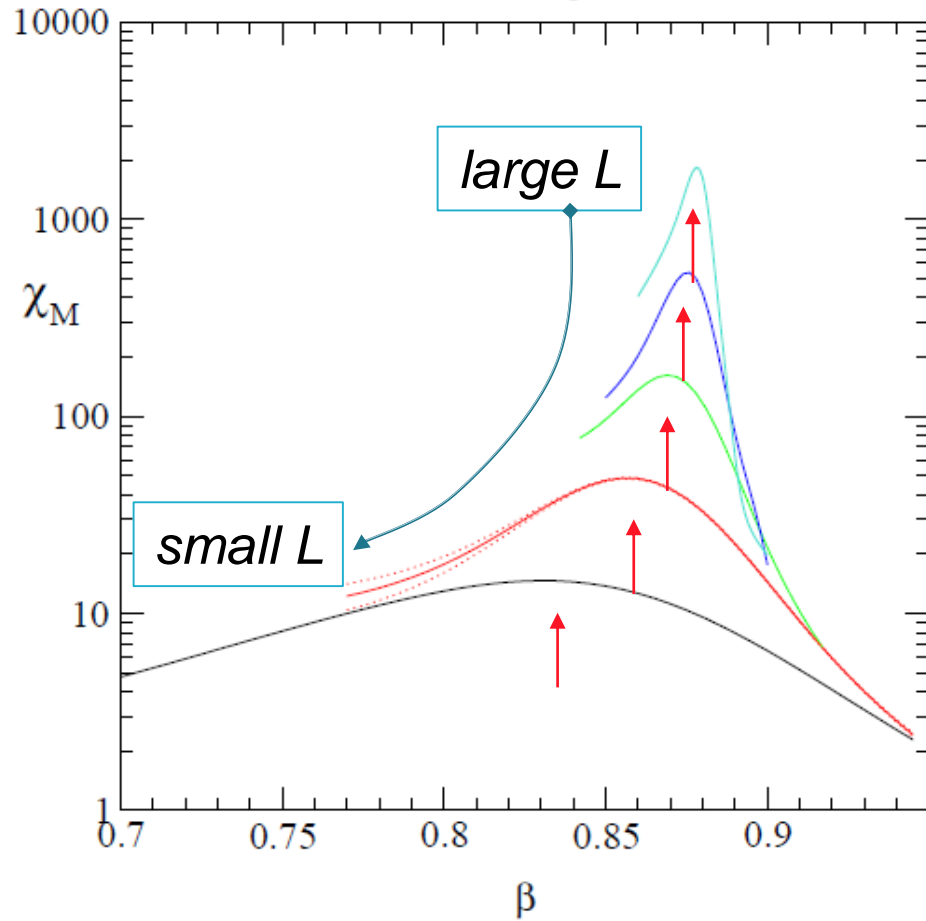
T close to T_c



$$\xi \sim |T - T_c|^{-\nu} \leq L$$

→ Only a pseudo-critical point is observed → shifted from the genuine CEP

$16^2 - 256^2$ Ising model



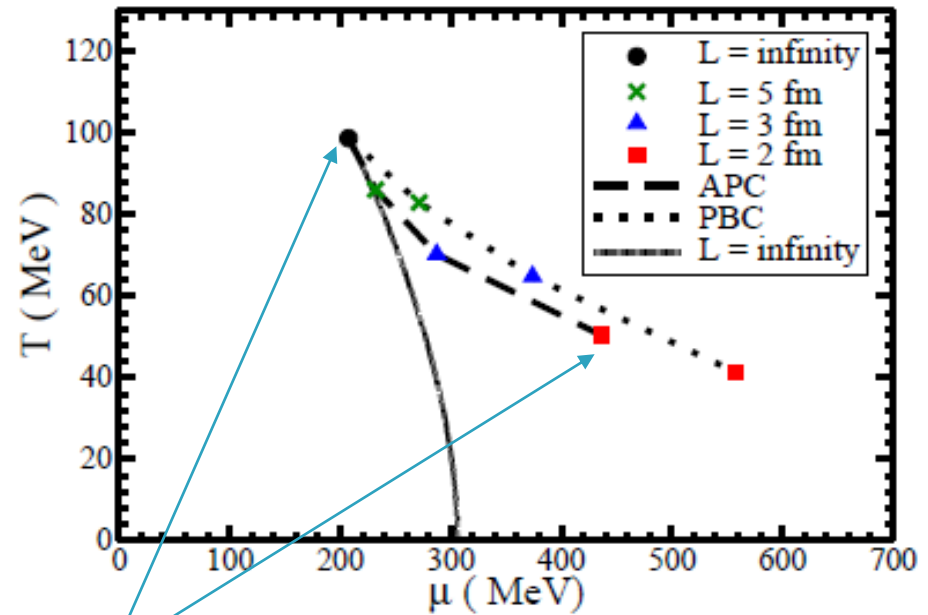
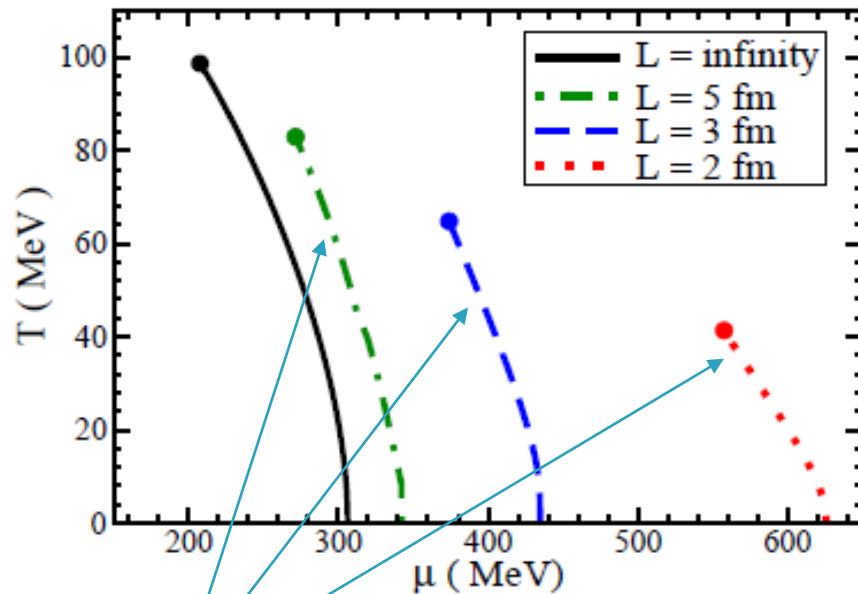
note change in peak heights, positions & widths

→ A curse of Finite-Size Effects (FSE)

The curse of Finite-Size effects

E. Fraga et. al.

J. Phys.G 38:085101, 2011



Displacement of pseudo-first-order transition lines and CEP due to finite-size

**Finite-size shifts both the pseudo-critical point
and the transition line**

*→ A flawless measurement, sensitive to FSE, **can not** give
the precise location of the CEP directly*

The Blessings of Finite-Size

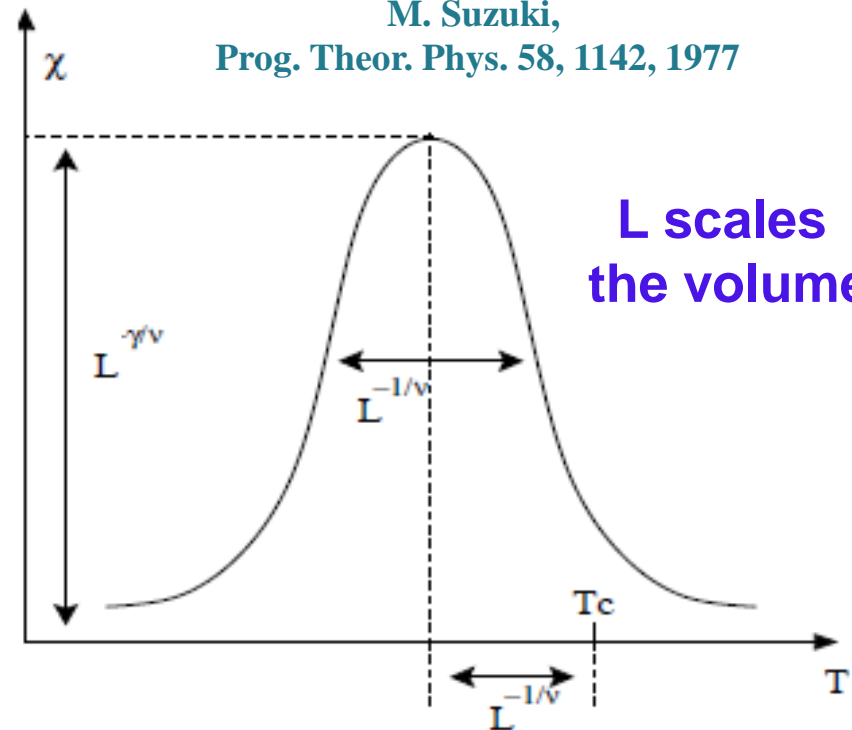
$$\chi_T^{\max}(V) \sim L^{\gamma/\nu},$$

$$\delta T(V) \sim L^{-\frac{1}{\nu}},$$

$$\tau_T(V) \sim T^{\text{cep}}(V) - T^{\text{cep}}(\infty) \sim L^{-\frac{1}{\nu}},$$

$$\chi(T, L) = L^{\gamma/\nu} P_\chi(tL^{1/\nu}) \quad t = (T - T_c) / T_c$$

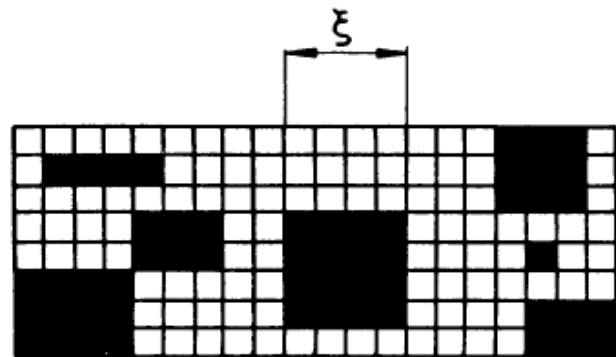
M. Suzuki,
Prog. Theor. Phys. 58, 1142, 1977



a) $T > T_c$

b) T close to T_c

Finite-size effects have a specific
L dependence



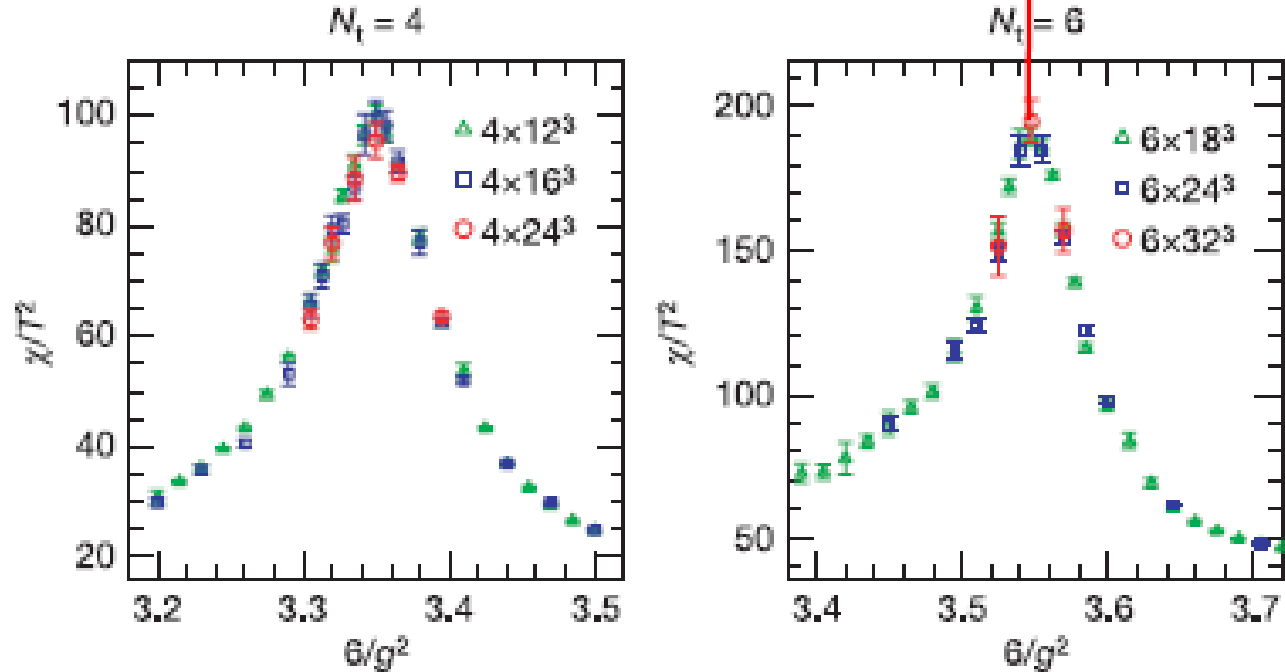
$$\xi \sim |T - T_c|^{-\nu} \leq L$$

- ✓ Finite-size effects have specific identifiable dependencies on size (L)
- ✓ The scaling of these dependencies give access to the CEP's location, it's critical exponents and scaling function.

Finite size scaling and the Crossover Transition

Finite size scaling played an essential role for identification of the crossover transition!

Y. Aoki, et. Al., *Nature*,
443, 675(2006).



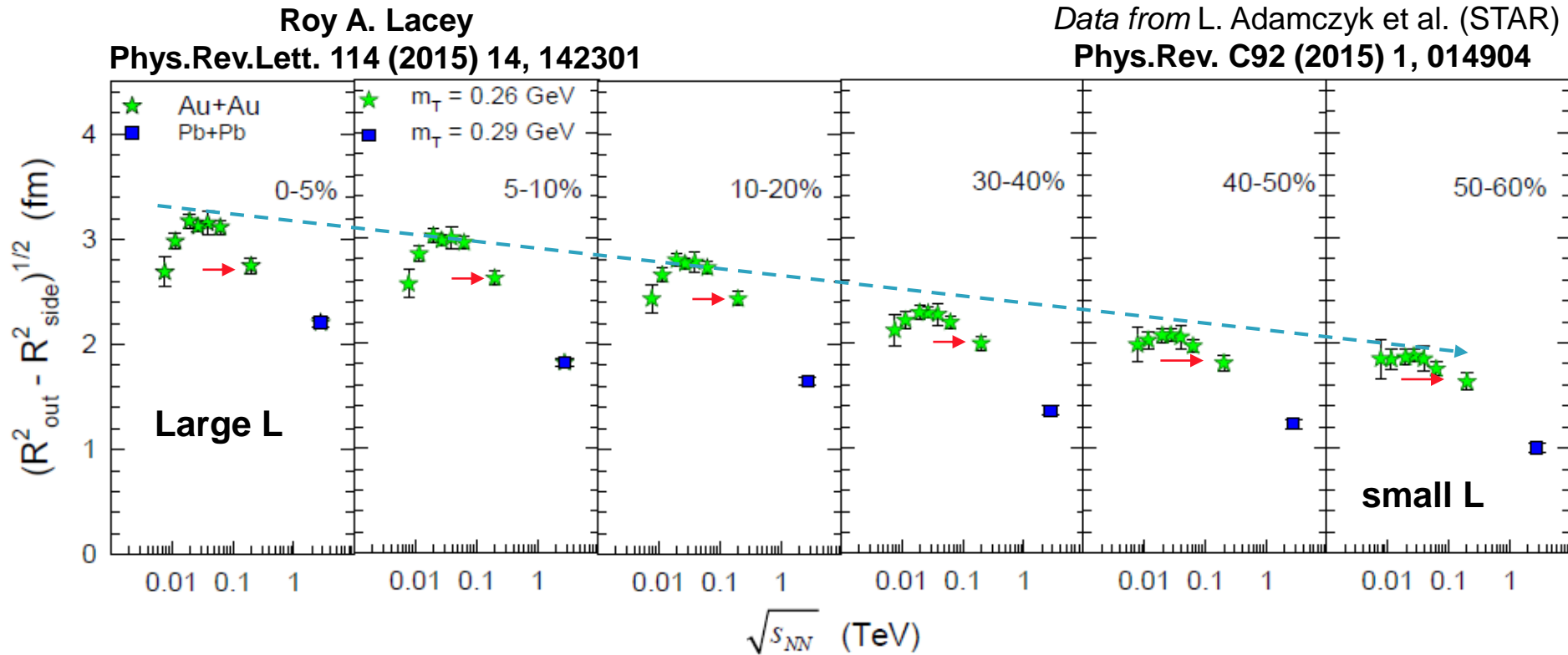
Reminder

Crossover: size independent.

1st-order: finite-size scaling function, and scaling exponent is determined by spatial dimension (integer).

2nd-order: finite-size scaling function $\chi(T, L) = L^{\gamma/\nu} P_\chi(tL^{1/\nu})$

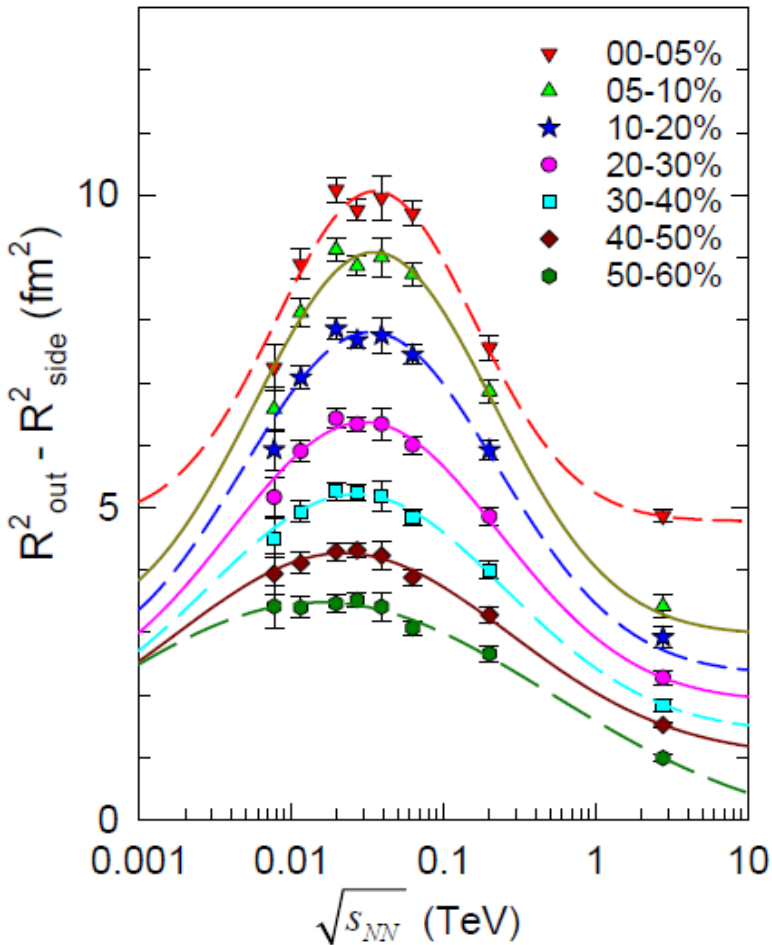
Size dependence of HBT excitation functions



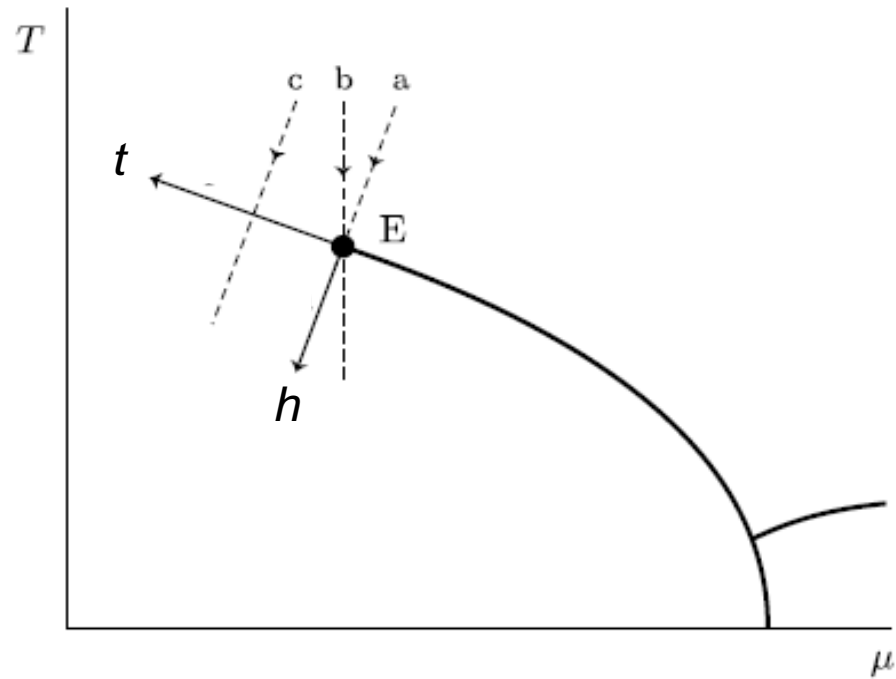
The data validate the expected patterns for Finite-Size Effects

- ✓ Max values decrease with decreasing system size
- ✓ Peak positions shift with decreasing system size
- ✓ Widths increase with decreasing system size

Size dependence of HBT excitation functions



characteristic patterns signal
the effects of finite-size



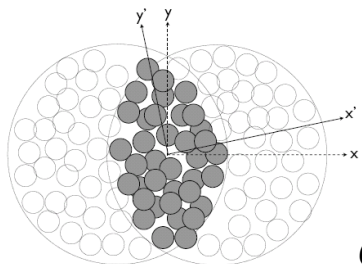
I. Use $(R_{out}^2 - R_{side}^2)$ as a proxy for the susceptibility

II. Parameterize distance to the CEP by $\sqrt{s_{NN}}$

$$\tau_s = (\sqrt{s} - \sqrt{s_{CEP}}) / \sqrt{s_{CEP}}$$

III. Perform Finite-Size Scaling analysis
with length scale $L = \bar{R}$

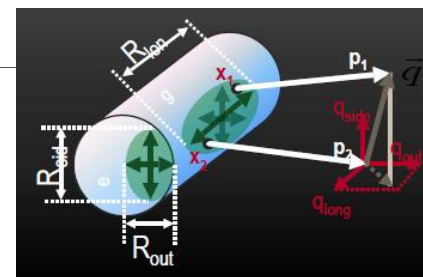
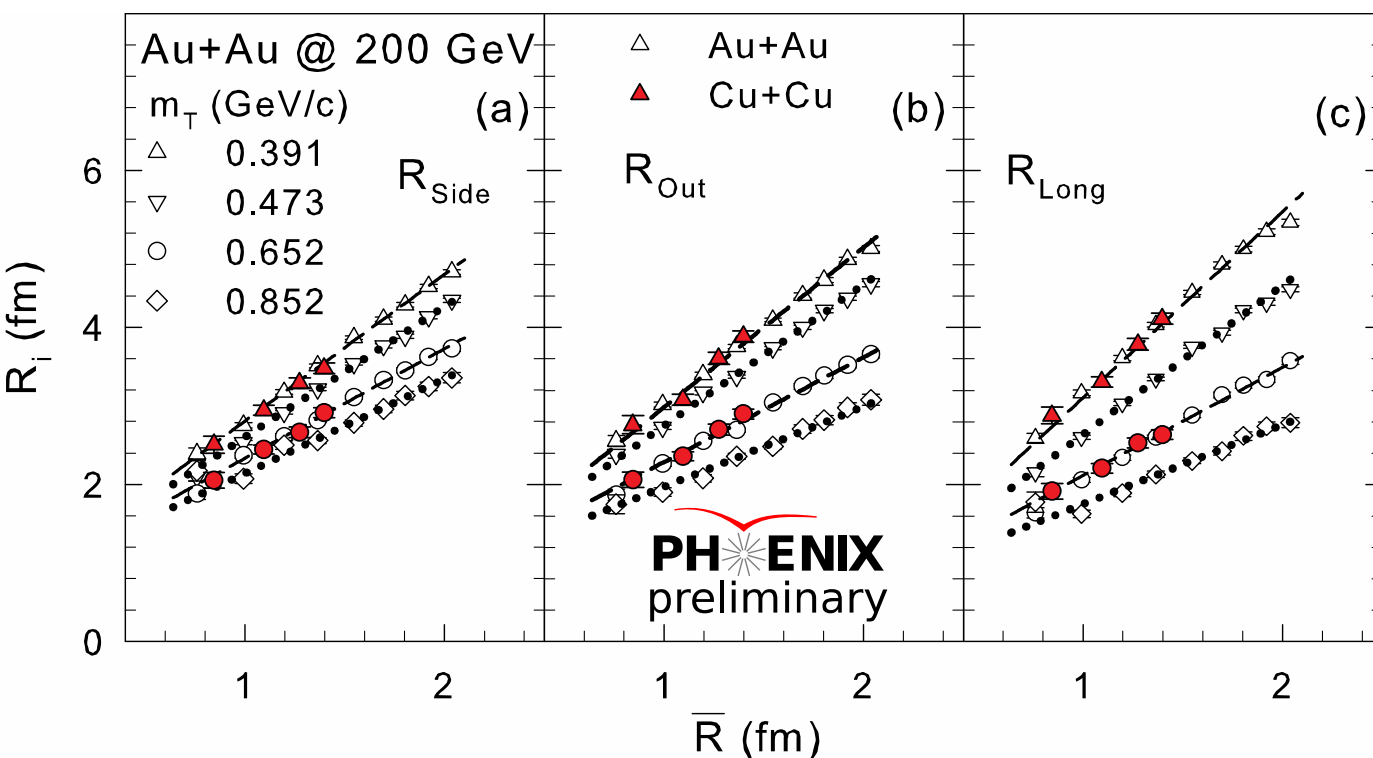
Length Scale for Finite Size Scaling



$$\frac{1}{\bar{R}} = \sqrt{\left(\frac{1}{\sigma_x^2} + \frac{1}{\sigma_y^2}\right)}$$

σ_x & $\sigma_y \rightarrow$ RMS widths of density distribution

\bar{R} is a characteristic length scale of the initial-state transverse size,



$$R_{out}, R_{side}, R_{long} \propto \bar{R}$$

\bar{R} scales the volume

\bar{R} scales the full RHIC and LHC data sets

Summary of Scaling Procedure

(only two exponents are independent)

$$\chi_T^{\max}(V) \sim L^{\gamma/\nu},$$

$$\delta T(V) \sim L^{-\frac{1}{\nu}},$$

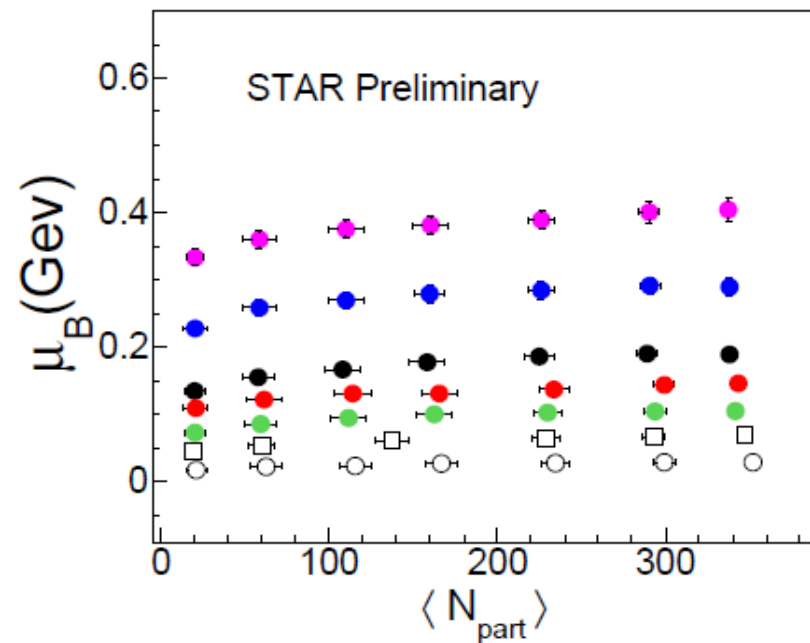
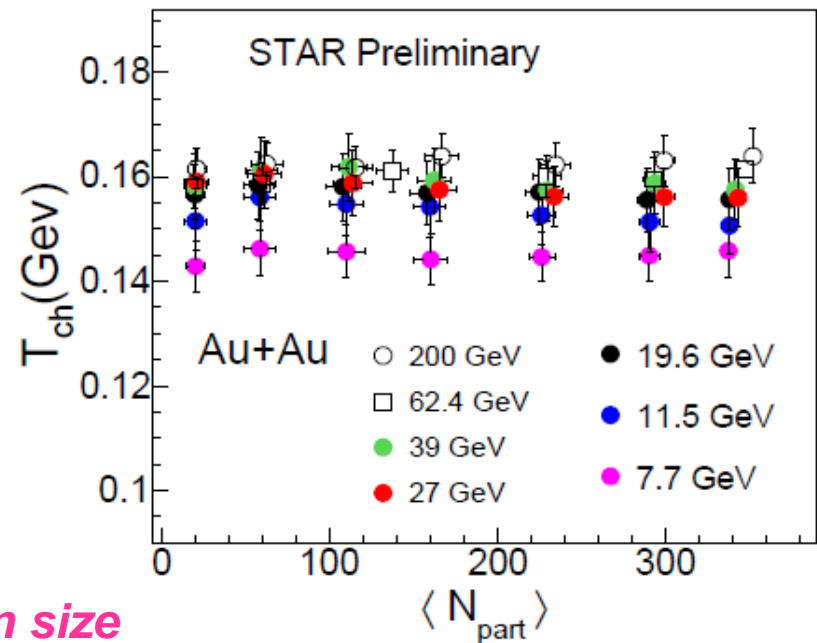
$$\tau_T(V) \sim T^{\text{cep}}(V) - T^{\text{cep}}(\infty) \sim L^{-\frac{1}{\nu}},$$

$$(R_{\text{out}}^2 - R_{\text{side}}^2)^{\max} \propto \bar{R}^{\gamma/\nu},$$

$$\sqrt{s_{NN}}(V) = \sqrt{s_{NN}}(\infty) - k \times \bar{R}^{-\frac{1}{\nu}},$$

Note that (μ_B^f, T^f) is not strongly dependent on size

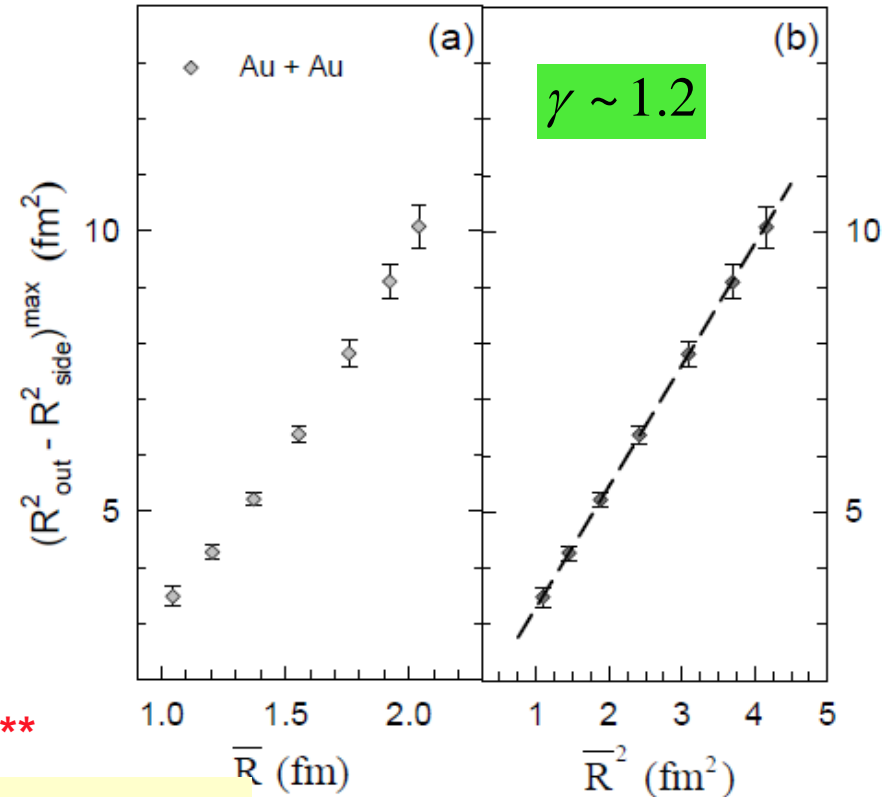
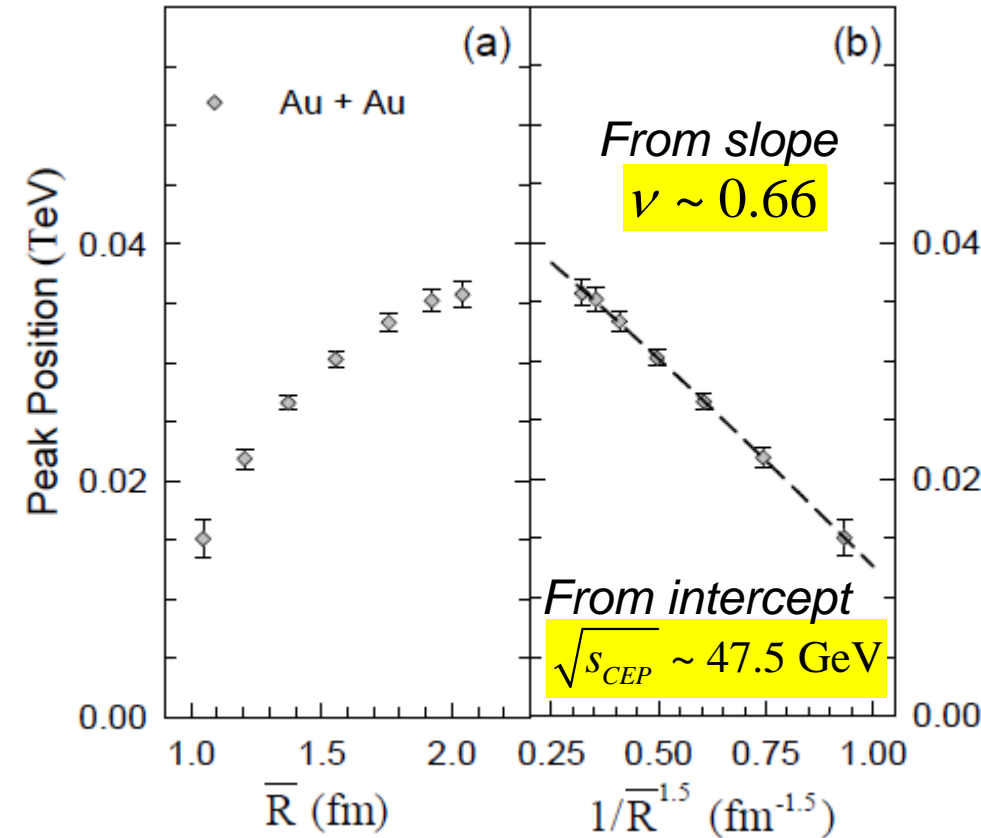
- Extract position ($\sqrt{s_{NN}}$) of deconfinement transition and critical exponents
- Use exponents to determine:
 - ✓ Order of the phase transition
 - ✓ Static universality class



Finite – Size Scaling

$$\sqrt{s_{NN}}(V) = \sqrt{s_{NN}}(\infty) - k \times \bar{R}^{-1/\nu}$$

$$(R_{out}^2 - R_{side}^2)^{max} \propto \bar{R}^{\gamma/\nu}$$



**** Same ν value from analysis of the widths ****

- **The critical exponents validate**
 - ✓ **the 3D Ising model (static) universality class**
 - ✓ **2nd order phase transition for CEP**

$$T^{cep} \sim 165 \text{ MeV}, \mu_B^{cep} \sim 95 \text{ MeV}$$

($\sqrt{s_{CEP}}$ & chemical freeze-out systematics)

Closer test for FSS

- 2nd order phase transition
- 3D Ising Model (static) universality class for CEP

$$\nu \sim 0.66 \quad \gamma \sim 1.2$$

$$T^{cep} \sim 165 \text{ MeV}, \mu_B^{cep} \sim 95 \text{ MeV}$$

$$\chi(T, L) = L^{\gamma/\nu} P_\chi(tL^{1/\nu})$$

M. Suzuki,

Prog. Theor. Phys. 58, 1142, 1977

Use T^{cep} , μ_B^{cep} , ν and γ
to obtain Scaling
Function P_χ

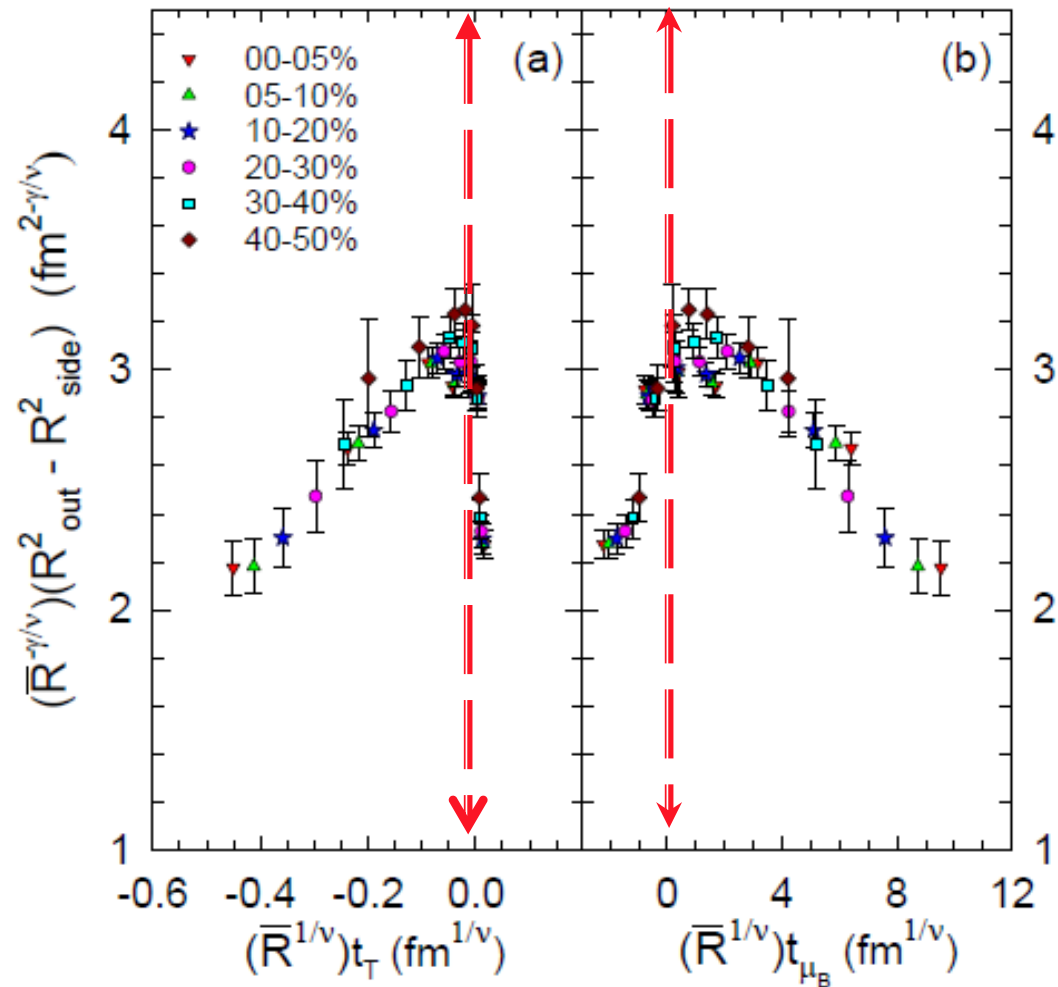
$$R^{-\gamma/\nu} \times (R_{out}^2 - R_{side}^2) \text{ vs. } R^{1/\nu} \times t_T,$$

$$\bar{R}^{-\gamma/\nu} \times (R_{out}^2 - R_{side}^2) \text{ vs. } \bar{R}^{1/\nu} \times t_{\mu_B},$$

$$t_T = (T - T^{cep})/T^{cep}$$

$$t_{\mu_B} = (\mu_B - \mu_B^{cep})/\mu_B^{cep}$$

T and μ_B are from $\sqrt{s_{NN}}$



****A further validation of the location of the CEP and the (static) critical exponents****

What about Finite-Time Effects (FTE)?

χ_{op} diverges at the CEP

so relaxation of the order parameter could be anomalously slow



$z > 0$ - Critical slowing down

Non-linear dynamics →

Multiple slow modes

$$z_T \sim 3, z_V \sim 2, z_S \sim -0.8$$

$z_S < 0$ - Critical speeding up

Y. Minami - Phys.Rev. D83 (2011) 094019

An important consequence

$$\xi \sim \tau^{1/z}$$

Significant signal attenuation for short-lived processes

with $z_T \sim 3$ or $z_V \sim 2$

eg. $\langle(\delta n)\rangle \sim \xi^2$ (without FTE)

$\langle(\delta n)\rangle \sim \tau^{1/z} \ll \xi^2$ (with FTE)

The value of the dynamic critical exponent/s is crucial for HIC

Dynamic Finite-Size Scaling (DFSS) is used to estimate the dynamic critical exponent z

Dynamic Finite – Size Scaling

➤ 2nd order phase transition

$$\nu \sim 0.66$$

$$\gamma \sim 1.2$$

$$T^{cep} \sim 165 \text{ MeV}, \mu_B^{cep} \sim 95 \text{ MeV}$$

DFSS ansatz

at time τ when T is near T_{cep}

$$\chi(L, T, \tau) = L^{\gamma/\nu} f(L^{1/\nu} t_T, \tau L^{-z})$$

$$t_T = (T - T^{cep})/T^{cep}$$

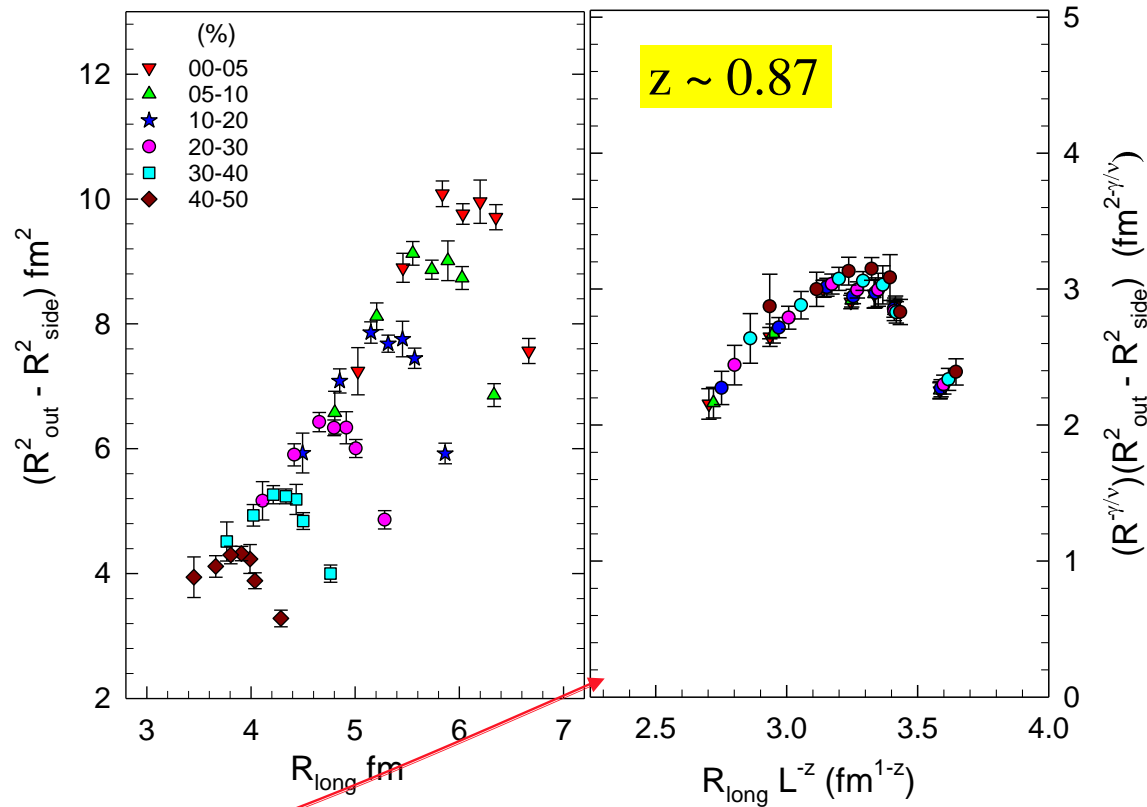
For
 $T = T_c$

$$\chi(L, T_c, \tau) = L^{\gamma/\nu} f(\tau L^{-z})$$

M. Suzuki,
Prog. Theor. Phys. 58, 1142, 1977

$$R_{long} \propto \tau$$

****Experimental estimate of the dynamic critical exponent****



The magnitude of z is similar to the predicted value for z_s but the sign is opposite

Epilogue

Strong experimental indication for the CEP and its location

(Dynamic) Finite-Size Scaling analysis

- 3D Ising Model (static) universality class for CEP
- 2nd order phase transition

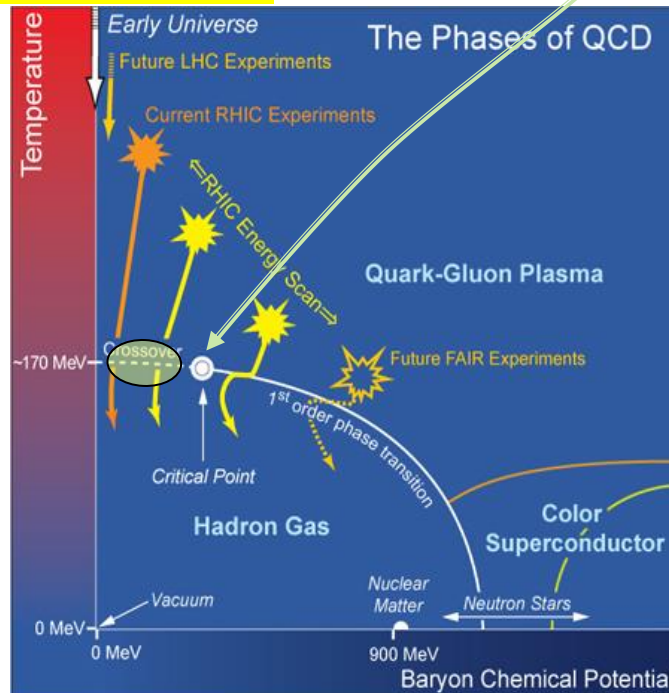
$$\nu \sim 0.66$$

$$\gamma \sim 1.2$$

$$z \sim 0.87$$

$$T^{cep} \sim 165 \text{ MeV}, \mu_B^{cep} \sim 95 \text{ MeV}$$

- ✓ Landmark validated
- ✓ Crossover validated
- ✓ Deconfinement validated
- ✓ (Static) Universality class validated
- ✓ Model H dynamic Universality class invalidated?
- ✓ Other implications!



New Data from RHIC (BES-II) together with theoretical modeling, can provide crucial validation tests for the coexistence regions, as well as to firm-up characterization of the CEP!



Much additional work required to get to “the end of the line”

End

Phys.Rev.Lett.100:232301,2008)

Source breakup dynamics in Au+Au Collisions at $\sqrt{s_{NN}}=200$ GeV via three-dimensional two-pion source imaging

S. Afanasiev,¹⁷ C. Aidala,⁷ N.N. Ajitanand,⁴³ Y. Akiba,^{37,38} J. Alexander,⁴³ A. Al-Jamel,³³ K. Aoki,^{23,37} L. Aphecetche,⁴⁵ R. Armendariz,³³ S.H. Aronson,³ R. Averbeck,⁴⁴ T.C. Awes,³⁴ B. Azmoun,³ V. Babintsev,¹⁴ A. Baldisseri,⁸ K.N. Barish,⁴ P.D. Barnes,²⁶ B. Bassalleck,³² S. Bathe,⁴ S. Batsouli,⁷ V. Baublis,³⁶ F. Bauer,⁴ A. Bazilevsky,³ S. Belikov,^{3,16,*} R. Bennett,⁴⁴ Y. Berdnikov,⁴⁰ M.T. Bjorndal,⁷ J.G. Boissevain,²⁶ H. Borel,⁸ K. Bratkovskii,⁴⁴ M. Bratkovskii,²⁶ D.S. Brown,³³ D. Brown,²⁹ H. Brune,³ V. Brune,¹⁴ C. Burchat,^{3,38}

Phys.Lett. B685 (2010) 41-46

Three-dimensional two-pion source image from Pb+Pb collisions at $\sqrt{s_{NN}}=17.3$ GeV: new constraints for source breakup dynamics

C. Alt⁹, T. Anticic²³, B. Baatar⁸, D. Barna⁴, J. Bartke⁶, L. Betev¹⁰, H. Białkowska²⁰, C. Blume⁹, B. Boimska²⁰, M. Botje¹, J. Bracinik³, P. Bunčić¹⁰, V. Cerny³, P. Christakoglou¹, P. Chung¹⁹, O. Chvala¹⁴, J.G. Cramer¹⁶, P. Csató⁴, P. Dinkelaker⁹, V. Eckardt¹³, D. Flierl⁹, Z. Fodor⁴, P. Foka⁷, V. Friese⁷, J. Gál⁴, M. Gaździcki^{9,11}, V. Genchev¹⁸, E. Gładysz⁶, K. Grebieszko²², S. Hegyi⁴, C. Höhne⁷, K. Kadija²³, A. Karev¹³, S. Kniege⁹, V.I. Kolesnikov⁸, R. Korus¹¹, M. Kowalski⁶, M. Kreps³, A. Laszlo⁴, R. Lacey¹⁹, M. van Leeuwen¹, P. Lévai⁴, L. Litov¹⁷, B. Lungwitz⁹, M. Makariev¹⁷, A.I. Malakhov⁸, M. Mateev¹⁷, G.L. Melkumov⁸,

$$\tau = \tau_0 + a\rho$$

Space-time correlation parameter

Interferometry as a susceptibility probe

Dirk Rischke and Miklos Gyulassy
Nucl.Phys.A608:479-512,1996

Fig. 1

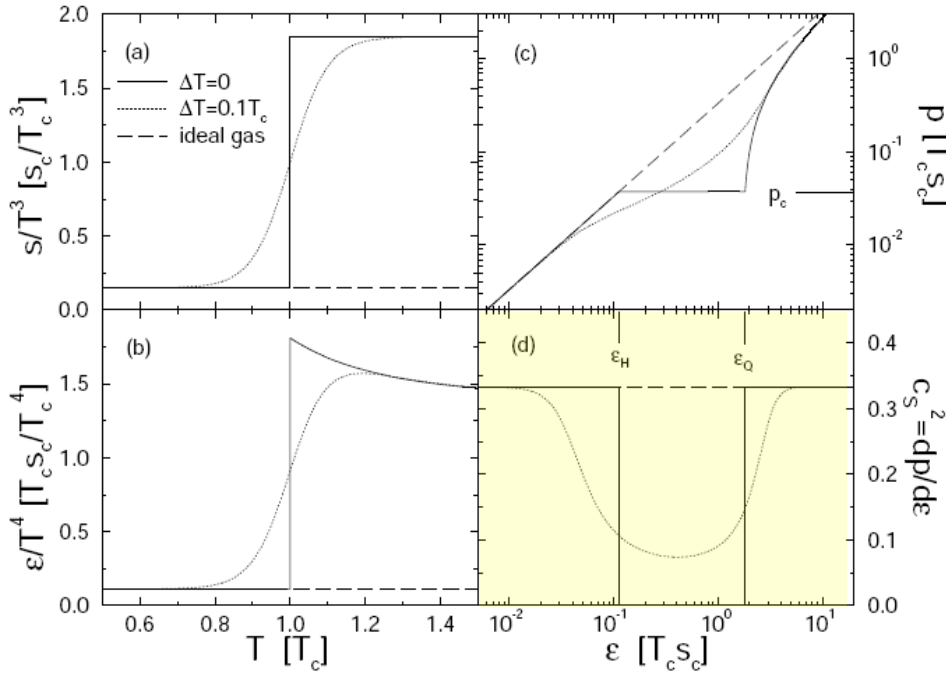
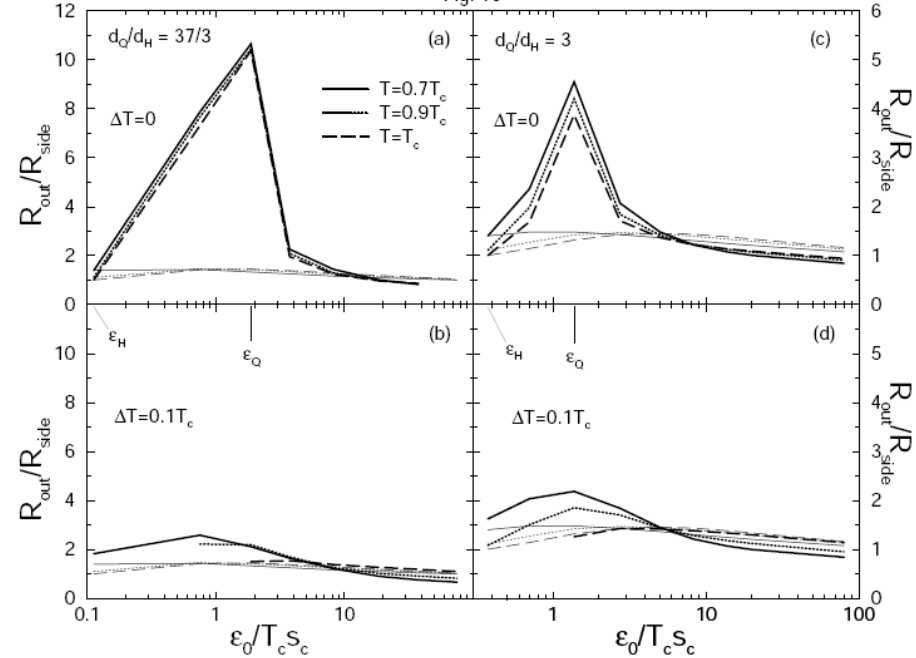


Fig. 16



In the vicinity of a phase transition or the CEP, the sound speed is expected to soften considerably.

$$c_s^2 = \frac{1}{\rho \kappa_s}$$

Divergence of the compressibility (κ)
→ non-monotonic excitation function for $(R_{out}^2 - R_{side}^2)$ due to an enhanced emission duration